Two Types of Ca^{2+}-channels in Cells from the Circular Layer of Guinea-pig Ileum

D. B. DURIDANOVA, H. S. GAGOV* and K. K.BOEV

Institute of Physiology, Bulgarian Academy of Sciences, Acad. G. Bonchеff Str., bl.23, 1113 Sofia, Bulgaria

Abstract. In this paper data are presented concerning some morphometrical characteristics and passive electrical properties of cell membranes from the circular layer of guinea-pig ileum (CC). The main purpose of the study has been to analyze the inward calcium current in these cells.

Using the whole-cell voltage-clamp method the presence of T-like type of calcium channels (conducting low-threshold, fast inactivated, strictly potential-dependent and dihydropyridine-resistant calcium inward current – I_f) could be found in membranes of the cells investigated. The participation of I_f in the total inward current of CC was deduced from the presence of a low-threshold "hump" in the current-voltage relation curve (I/V-curve) between -80 and -50 mV, and also from a negative shift of this curve at holding potential $V_h = -90$ mV, compared to the one obtained at $V_h = -50$ mV. Besides, in the presence of a dihydropyridine Ca^{2+} antagonist, a fast inactivating component of the inward current could be recorded, which was effectively blocked by 0.3 mmol/l Ni^{2+} from outside. According to Tsien's criteria (1983) our data suggest the coexistence of T- and L-types calcium channels in CC.

Key words: Calcium channels — Smooth muscle — Ileum — Guinea-pig — Whole-cell voltage clamp — T-current

Introduction

Quite many publications, dealing with the regulation of Ca^{2+} currents in smooth muscle cells, including those, isolated from the guinea-pig ileum, have appeared lately (see for example Somlyo and Somlyo 1992; Suzuki et al. 1992). Earlier voltage-clamp studies in ileal cells provide no exact information on the smooth muscle layer, from which the cells had been isolated (Droogmans and Callewaert 1986; Zholos et al. 1992). The lack of a systematic and consistent description of

* Correspondence to Dr. H. Gagov

the individual components of the inward and outward currents in these cells is also evident.

A huge amount of knowledge has accumulated in recent years concerning the existence of two different types of calcium channels, operating in membranes of smooth muscle cells from visceral organs (Yoshino et al. 1988; Miyoshi et al. 1991; Yamamoto et al. 1988; Isenberg et al. 1992). The first, widely distributed L-type (high threshold, long lasting, dihydropyridine-sensitive) Ca^{2+}-channel seems to be omnipresent in the membranes of smooth muscle cells, including those from intestinal smooth muscles (Pelzer et al. 1990; Yamamoto et al. 1989; for review, see Spedding and Kenny 1992). The characteristics of the second, low-threshold fast inactivating and strictly potential dependent calcium channel type, described in the myometrium (Miyoshi et al. 1991), the ureter (Isenberg and Klockner 1985) and the vas deferens (Nakazawa et al. 1988) have been compared to type I (T-type) Ca^{2+} channel known to be present in the heart (Nilius et al. 1985), vessel muscles (Benham et al. 1987) and neuronal membranes (Nowycky et al. 1984). In some smooth muscle cells isolated from the gastrointestinal tract a fast, time-dependent component of the inactivation of the whole-cell current was registered; it was dihydropyridine resistant, but highly sensitive to submilimollar concentrations of Ni^{2+} (Yoshino and Yabu 1985; Vogalis and Sanders 1991; Post and Hume 1992). A low-threshold strictly potential dependent Ca^{2+} current component was also recorded, forming a "hump" on the current-voltage (I/V) curve for total inward current, which dissapeared in the presence of Ni^{2+} (Yoshino et al. 1988; Duridanova et al. 1992). According to the Tsien's criteria (Tsien 1983) this data should be accepted as a sufficient proof of the presence of T-type channel activity in these tissues (Isenberg et al. 1992). However, there are some difficulties in obtaining convincing data about the existence of T-type calcium channels in intestinal smooth muscle cells: a) it is impossible to obtain "pure" current through T-channels (the steady-state activation and inactivation characteristics of L- and T-types channels have quite large areas of overlapping in these tissues, see Bolton and Pacaud 1992); b) research work on ion currents of pacemaker cells in these organs has been very limited due to the difficult identification of the cells during isolation procedures, see Ward et al. (1991) and, c) there is a lack of a clear understanding of the physiological function of the low-threshold Ca^{2+}-channels for the electro-mechanical coupling in intestinal smooth muscle.

This paper presents data on some morphometrical characteristics and passive electrical properties of cells isolated from the circular layer of the guinea-pig ileum (CC), and on the characteristics of the calcium inward current in the membranes of these cells; to the best of our knowledge, these cells have not yet been analyzed in this respect. The results obtained suggest the presence of a T-like type of Ca^{2+}-channel in CC.

Table 1. Composition of bath solutions (in mmol/l)

	A	B	C (PSS)	D	E
NaCl	135.0	120.0	115.0	110.0	105.0
KCl	5.0	12.0	12.0	12.0	12.0
$MgCl_2$	2.0	1.2	1.2	1.2	1.2
Glucose	10.0	20.0	20.0	20.0	20.0
Taurine	0.0	20.0	20.0	20.0	20.0
HEPES*	10.0	10.0	10.0	10.0	10.0
Pyruvate	0.0	5.0	5.0	5.0	5.0
$CaCl_2$	0.0	0.0	2.5	0.0	2.5
TEA-Cl**	0.0	0.0	0.0	10.0	10.0

* N-2-hydroxyethylpiperazine-N′-2-ethanesulfonic acid. pH of all solutions was adjusted with KOH to 7.35–7.4

** Tetraethylammonium chloride

Materials and Methods

Guinea pigs of either sex, weighing 200–250 g, were used. Strips of 5 mm length were removed from the circular muscle layer of the terminal ileum and placed in separate Petri dishes, containing Ca^{2+}-free solution for cell isolation (solution A, Table 1). The muscle strips were cut into pieces, 2.5 mm in length, and incubated in an enzyme-dispersing medium (solution B, Table 1) with 0.5 g/l collagenase (165 U/mg, type IA, Sigma Chemicals Co, St. Louis, MO), 1.5 g/l soybean trypsin inhibitor (type II-S, Sigma T9128) and 2 g/l bovine serum albumine (fraction V, SERVA, cat. No 11922). After incubation at 37 °C for 30 min with gentle stirring and bubbling with O_2, the dispersing medium was replaced by fresh solution B, kept at 30–32 °C, in five separate washes. After the last wash the tissue pieces were resuspended in modified "KB" medium (see Isenberg and Klockner 1982) in four separate washes, then placed into a cuvette and triturated with a glass Pasteur pipettes with two different tip openings (1.8 mm and 0.9 mm). The modified "KB" solution consisted of (in mmol/l): 85 KCl, 30 KH_2PO_4, 20 taurine, 5 $MgCl_2$, 10 glucose, 1 EGTA, 2.2 Na_2-ATP (disodium salt of adenosine triphosphate), 5 succinic acid, 5 pyruvic acid, sodium salt, 5.3 creatine, 1% bovine serum albumin; pH adjusted to 7.2. After trituration the material was filtered through a 250 μm nylon mesh to remove undispersed fragments. The cell suspension thus obtained was stored in cold for up to 24 hours. For the purpose of the study, only fully relaxed cells were used. The material was drawn from these stocks and placed into the experimental chamber. Cells, which reduced their length by more than 35% or did not contract at all after application of 10^{-7} mol/l acetylcholine, were discarded, as were those which did not relax after acetylcholine-induced contraction.

Electrophysiological techniques

The patch-clamp technique and whole-cell configuration was employed (Hamill et al. 1981). Electrodes were made from borosilicate glass, 1.45 mm o.d. (Jencons Scientific Ltd., Leighton Buzzard) and heat-polished on a microforge to final tip opening of

Table 2. Composition of pipette solution* (in mmol/l)

	K^+	Cs^+
KCl	105 0	0 0
CsCl	0 0	105 0
HEPES	10 0	10 0
EGTA**	11 0	11 0
$MgCl_2$	2 0	2 0
$CaCl_2$	1 0	1 0
Glucose	14 0	14 0

* To 5 ml of this solution, used as a stock, were added immediately before use (in mmol/l) 4 pyruvic acid sodium salt, 4 succinic acid, 4 oxalacetic acid, 1 5 adenosine triphosphate sodium salt, 0 001 cyclic adenosine monophosphate sodium salt, pH adjusted to 7 2–7 3 with KOH

** Ethylene glycol-bis-(-amino ethyl ether) N,N′ tetraacetic acid

1 5 2 0 μm in diameter The resistance of the electrode filled with intracellular solution (standard K^+-pipette solution, Table 2) was about 1 MΩ The experimental chamber consisted of a 10 mm square dish with a glass coverslip at the bottom, to which the dispersed cells usually adhered after a 20 min settling time All experiments were performed at 30–32 °C Temperated solutions (Table 1) were continuously and separately perfused into the chamber at a rate of 0 7 ml/min The experimental chamber was observed under a light microscope (magnif 1000x) connected to a CCD-camera (Nikon) and displayed on a TV-screen (14″) using a VHS video-recorder

A List EPC-7 amplifier was used Giga-ohm seals (usually 5–10 GΩ) were established by the usual suction method (Hamill et al 1981) Pulsative suctions were used to break the membrane in the micropipette tip The signals were digitized by the use of a Labmaster TL-1 interface (Axon Instruments Inc) Data analyses were performed with the use of an IBM/AT 16-bit microcomputer and pCLAMP software

Results

General description

In cold "KB" solution (8 °C) most cells are elongated and fully relaxed In 2 5 mmol/l external Ca^{2+} - $[Ca^{2+}]_o$ - (physiological salt solution - PSS - or solution C from Table 1), they tend to contract

The morphometrical and capacitive parameters were measured in cold "KB" solution and are summarized in Table 3 The estimated visible cell surface area (S_v) was in good accordance with the capacitive surface area (S_c), assuming 1 $\mu F/cm^2$ as specific membrane capacitance The difference between values estimated by these procedures was 10–12% The average $(S_v + S_c)/2$ values obtained are shown in Table 3

Table 3. Parameters of cells isolated from the circular layer of the guinea-pig ileum*

Surface area (μm^2)	Visible length (μm)	Visible diameter (μm)	Capacitance (pF)
7125 ± 268	251 ± 29	11.0 ± 0.5	70.75 ± 8.31

* Data are means ± S.E.M. for 169 cells

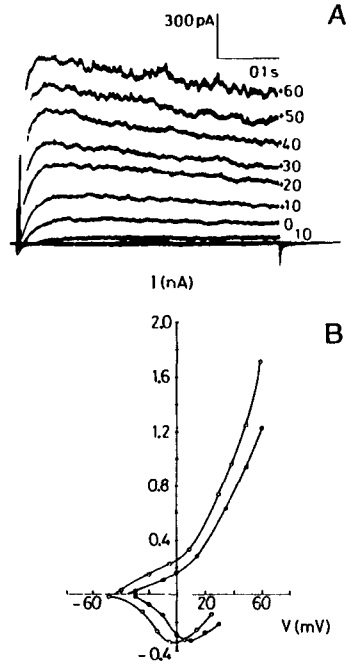

Figure 1. Whole-cell responses of a cell with input impedance 1.7 GΩ and capacitance 63.4 pF under voltage clamp (*A*). PSS, K^+-pipette solution. Voltage steps in mV. $V_h = -50$ mV. (*B*) *I/V*-relation curves of inward and outward currents, elicited by depolarization steps from $V_h = -90$ mV (open circles) and $V_h = -50$ mV (filled circles), K^+-pipette solution. Data are means for 6 cells. Standard deviation bars are not shown. The amplitudes of the inward and outward currents were measured simultaneously at each depolarizing stimulus.

A value of -49 ± 5.6 mV ($n = 67$) was found for the resting potential (V_r). V_r was always measured in PSS and with K^+ solution in the pipette.

Total membrane currents. Fig. 1*A* shows the characteristic responses of CC in 2.5 mmol/l $[Ca^{2+}]_o$ (solution C). In the voltage-clamp mode, depolarizing steps produced the usual waveforms of an initial inward current (I_{Ca}), followed by a more sustained outward current, with a considerable overlap. The *I/V* relation curves for the whole-cell inward and outward currents are shown in Fig. 1*B*.

Inward current and its current-voltage relations. To study the inward current in detail, the K^+-outward current was blocked by 105 mmol/l CsCl as the pipette solution (Cs^+-solution, Table 2), instead of KCl and 10 mmol/l TEA outside (solutions D or E, Table 1). The amplitude of the inward current tended to decline with time ("run-down"). The "run-down" was generally noted within 40–60 min. Based on the data given in Table 3, the density of I_{Ca} was estimated to be 10.11 $\mu A/cm^2$, assuming a mean amplitude of the peak current of 720 pA (see below). Figs. 2 and 3 show typical I/V-curves of maximal I_{Ca} in $[Ca^{2+}]_o = 2.5$ mmol/l, obtained at two different holding potentials (V_h) : −50 mV (Fig. 2) and −90 mV (Fig. 3). These results are representative for this type of cells.

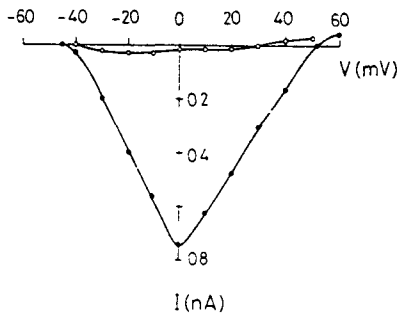

Figure 2. I/V-relations for peak I_{Ca} (filled circles) in solution E and in the presence of $3 \cdot 10^{-6}$ mol/l nifedipine (open circles) in a cell with 67.8 pF membrane capacitance and 1.8 GΩ input impedance Cs^+ pipette solution. $V_h = -50$ mV. The rectangular depolarizing stimuli applied had a duration of 400 ms

In cells voltage-clamped at $V_h = -50$ mV (Fig. 2, filled circles), the inward current was first detectable at -43 ± 3 mV. An average maximum amplitude of 0.72 ± 0.08 nA was reached at 0 mV test potential. The reversal potential was $+57 \pm 6$ mV ($n = 14$). At $V_h = -90$ mV (Fig. 3*A*, filled circles) the inward current became visible at about -75 ± 3 mV, showed a small "hump" on the I/V-curve at about −50 mV, and increased with depolarization, reaching its maximum at -12 ± 3 mV. The average maximum amplitude was 0.73 ± 0.04 nA. The reversal potential was $+52 \pm 4$ mV ($n = 9$).

I_{Ca} in the presence of nifedipine. At $V_h = -50$ mV nifedipine ($3 \cdot 10^{-6}$ mol/l) effectively inhibited I_{Ca} in the whole potential range tested (Fig. 2, open circles and Fig. 3*A*, squares). In cells voltage-clamped at $V_h = -90$ mV (Fig. 3*A*, open circles), the same concentration of the drug had little effect on I_{Ca} in the potential range from −80 to −45 mV, and showed a marked blocking potency on I_{Ca}, promoted by higher depolarizations. The low-threshold nifedipine-resistant component (inset in Fig. 3*A*) was totally blocked by 0.3 mmol/l Ni^{2+} applied from outside (Fig. 3*B*).

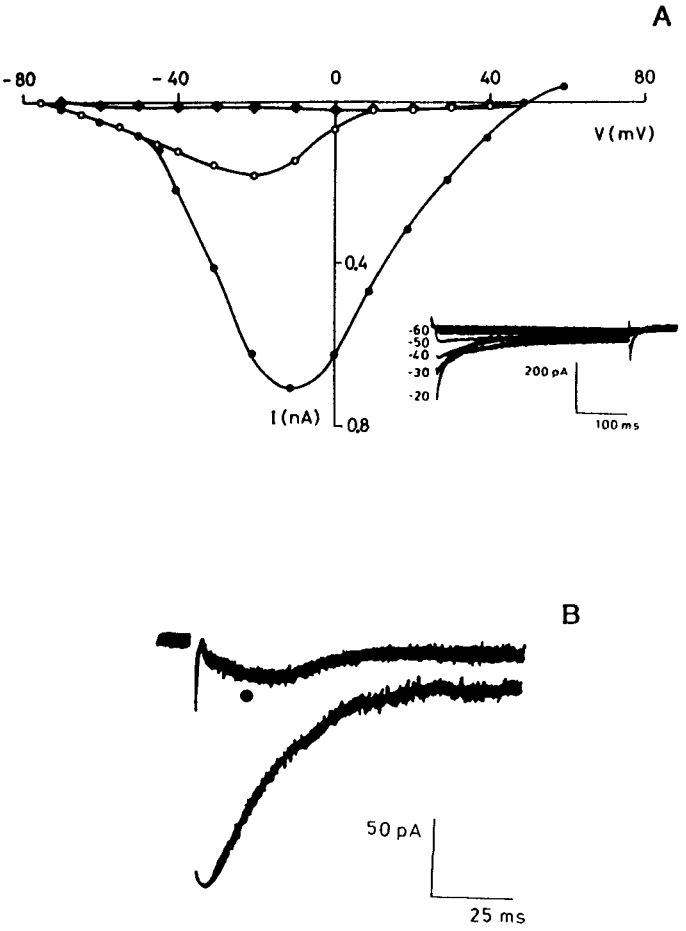

Figure 3. (*A*) I/V-relation curve for peak I_{Ca} (filled circles) and the blocking properties of $3 \cdot 10^{-6}$ mol/l nifedipine (open circles); a cell voltage-clamped at $V_h = -90$ mV. The effect of the same dose of nifedipine on I_{Ca} obtained under $V_h = -50$ mV (squares) is shown for comparison. Note the total block of I_{Ca} by the drug at $V_h = -50$ mV, and the presence of a low-threshold nifedipine-resistant current, forming a "hump" on the I/V-relation curve at $V_h = -90$ mV. Inset: Nifedipine/resistant current waveforms elicited by depolarizations from $V_h = -90$ mV to potentials shown, recorded from the same cell (capacitance 64.7 pF and 1.4 GΩ input impedance). (*B*) The effect of 0.3 mmol/l $NiCl_2$ on the nifedipine/resistant component of I_{Ca} (solution E + $3 \cdot 10^{-6}$ mol/l nifedipine). The same cell as in (*A*) . $V_h = -90$ mV. A depolarizing stimulus to −20 mV was applied. The I_{Ca} waveform recorded 3 min after the addition of $NiCl_2$ is marked by a circle.

Charge carrier. Fig. 4 shows some typical records in nominally Ca^{2+}-free medium (solution D) and in the presence of 2.5 mmol/l Cd^{2+} (added to solution E). The

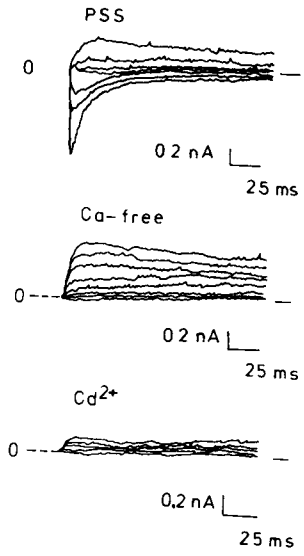

Figure 4. The influence of Ca^{2+}-free solution and of the exchange of $CaCl_2$ for an equimolar quantity of $CdCl_2$ on I_{Ca} in a cell with a capacitance of 59 pF and an input impedance of 1 2 GΩ $V_h = -90$ mV Depolarizing pulses were applied in 20 mV increments up to +90 mV (upper and middle trace), and to +110 mV (bottom trace) Some records have been omitted for the sake of clarity Upper trace control records obtained in solution E Middle trace the same cell in solution D Bottom trace 2 5 mmol/l $CdCl_2$ added into solution D

absence of Ca^{2+} in the bath solution led to a total abolishment of the inward current, while the outward current persisted and showed a tendency for increasing, especially at large depolarizations (Fig 4, middle trace) The application of 3 10^{-7} mol/l tetrodotoxin (TTX) was without any effect on the inward currents With 2 5 mmol/l $CdCl_2$ added into the bath the inward currents were completely blocked, and the outward current, elicited by large depolarizations, was significantly reduced (Fig 4, bottom trace)

Barium currents Fig 5 shows original recordings of the inward currents, carried by 2 5 mmol/l Ba^{2+} (solution D with $BaCl_2$) Ba^{2+} currents (I_{Ba}) showed similar I/V relationship as did I_{Ca} The peak I_{Ba} was 0 79 ± 0 03 nA in amplitude at $V_h = -50$ mV, and 0 69 ± 0 04 nA at $V_h = -90$ mV ($n = 8$) At $V_h = -90$ mV the "hump" on the I/V-curve remained within the same potential range as in Ca^{2+}-containing solution The I/V-relation curve at $V_h = -50$ mV was shifted 5 to 10 mV towards more positive voltages (Fig 5*C*) Note the presence of a fast decaying component with an amplitude of about 1/3 of the maximum at −40 mV test potential (from $V_h = -90$, Fig 5*B*), which reached its maximum in about 15–20 ms and was almost completely inactivated at the end of the pulse Replacement of Ca^{2+} with Ba^{2+} in our experiments could not significantly affect the maximum amplitudes of inward curents, but had a marked effect on their inactivation kinetics (see below) The reversal potentials of I_{Ba} could not be reached at all, even at high depolarization

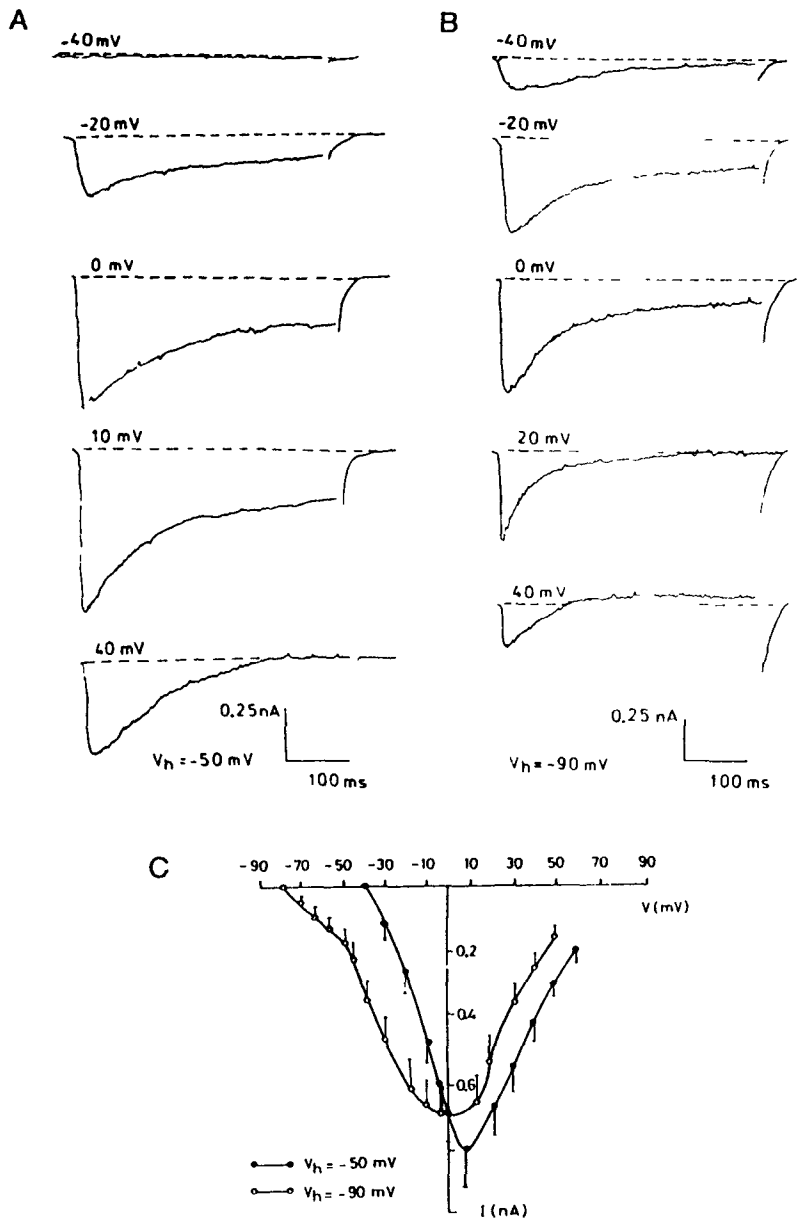

Figure 5. Barium currents through calcium channels, elicited by rectangular depolarizing stimuli from $V_h = -50$ mV (A) and $V_h = -90$ mV (B) to potentials shown (solution D with 2.5 mmol/l $BaCl_2$). Cell capacitance 70.0 pF, input impedance 1.9 GΩ. (C) Effect of V_h on I/V-relations for I_{Ba}. Data are means ± S.E.M. for 11 cells.

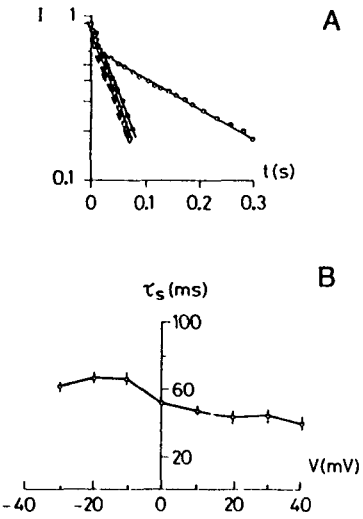

Figure 6. (*A*) Inactivation of the low- and high-threshold components of I_{Ca}. The inactivation of I_f was measured at −20 mV from V_h = −90 mV in solution E (filled triangles), in the same solution in the presence of $3 \cdot 10^{-6}$ mol/l nifedipine (filled circles), and in solution D with 2.5 mmol/l $BaCl_2$ (open triangles). The open circles represent the inactivation course of I_s, measured at 0 mV test potential under V_h = −50 mV in Ba^{2+}-containing solution D. Inactivation time courses plotted in semilogarithmic coordinates. Fits for the low-threshold component are monoexponential with τ_f = 21.5 ms in Ca^{2+}, 22.2 ms in Ba^{2+}, and 20.9 ms in the presence of nifedipine. For the high-threshold component τ_s = 228.2 ms (in Ba^{2+}). (*B*) Effect of membrane potential on time constants of inactivation τ_s in solution E. Symbols represent means ± S.E.M. for 9 cells.

Inactivation

Kinetics of inactivation. In solution E with the depolarizing step maintained, I_{Ca} declined after reaching a maximum, and inactivation was nearly complete in 2 s. The time course of inactivation of I_{Ca}, elicited by depolarization from V_h = −90 mV was complex, consisting of two exponential terms (Fig. 6). The first (I_f) had a time constant of inactivation $\tau_f = 21.5 \pm 1.3$ ms in solution E (n = 13) (Fig. 6*A*, filled triangles), and 22.4±2.1 ms in 2.5 mmol/l $[Ba^{2+}]_o$ (n = 9) (Fig. 6*A*, open triangles). Nifedipine did not affect the inactivation kinetics of this component (Fig. 6*A*, filled circles). The second, slow-inactivating component (I_s) had a time constant of inactivation $\tau_s = 235.03 \pm 8.7$ ms in 2.5 mmol/l $[Ba^{2+}]_o$ (n = 13) (Fig. 6*A*, open circles). In 2.5 mmol/l $[Ca^{2+}]_o$ the inactivation of the slow component of the peak I_{Ca} was accelerated about 4 times (Fig. 6*B*), reaching $\tau_s = 53 \pm 5.2$ ms at 0 mV (n = 14). The time constants τ_s showed a weak dependence on the test potential applied from V_h = −50 mW in Ca^{2+}-containing media.

Steady-state inactivation. The availability of the slow component of I_{Ca} − (I_s) − was investigated as a function of the membrane potential by a double pulse protocol. Fig. 7 shows the average steady-state inactivation data for I_s (open circles) and I_f (filled circles), obtained in solution E (data are means ± S.E.M. for 11 cells). The availability curve of the fast component was obtained in the presence of $3 \cdot 10^{-6}$ mol/l nifedipine. The $V_{1/2}$ of I_s was found to be -27.25 ± 2 mV, with slope factor $k_s = 6.79 \pm 0.4$ mV (mean ± S.E.M). The $V_{1/2}$ for I_f was -50.3 ± 3 mV, and the slope of this curve was $k_f = 6.61 \pm 0.3$ mV (mean ± S.E.M). The h_∞-curve of I_f

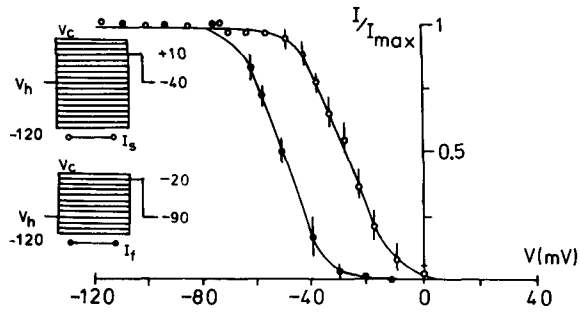

Figure 7. Steady-state inactivation of I_f (filled circles) and I_s (open circles) components of I_{Ca} in PSS. Data are means ± S.E.M. for 11 cells. Availability of I_f was obtained in the presence of $3 \cdot 10^{-6}$ mol/l nifedipine. Double-pulse protocol for I_s: conditioning stimuli (V_c) – 3 s, test stimulus (V_t) – 300 ms, $V_h = -40$ mV. For I_f : V_c of 3s duration, V_t – 40 ms, $V_h = -90$ mV. Steady-state inactivation was measured as the ratio I/I_{max}, where I_{max} is the maximum current amplitude during the V_t after the most hyperpolarizing conditional pulse. The −120 mV prepulse protocol followed each double-pulse complex as its own control to account for the "run-down" of I_{Ca}. A 30 s interval between series was allowed for full recovery of both components of I_{Ca}. The current ratios were plotted as a function of the prepulse potential. Smooth lines represent the fits according to the equation: $h_\infty = \{1 + \exp[(V_c - V_{1/2})/k]\}^{-1}$, where $h_\infty = I/I_{max}$, V_c is the conditioning potential, $V_{1/2}$ is the half-inactivation potential, and k is the slope factor. Estimated: $h_\infty(I_f) = \{1 + \exp[(V_c + 50.3)/6.61]\}^{-1}$, and $h_\infty(I_s) = \{1 + \exp[(V_c + 27.25)/6.79]\}^{-1}$.

showed a pure voltage dependence of its inactivation. The estimated $V_{1/2}$ of I_s suggests that about 50% of I_f is inactivated at a potential 15 mV positive to its activation threshold (see Fig. 2).

Discussion

Two types Ca^{2+}-currents in CC. The slow component I_s of I_{Ca} analyzed above has previously been described in many objects, including cells from the longitudinal layer of the same organ (see Droogmans and Callewaert 1986; Duridanova et al. 1992). It was confirmed by a number of experimental paradigms and was thought to be carried through L-type Ca^{2+}-channels. But the data obtained in the present studies allowed us to suggest the presence of another type of Ca^{2+}-channel in CC as well. The difficulties associated with all previous attempts to unequivocally separate putative currents through L- and T-type Ca^{2+}-channels have been reported (for review see Bolton and Pacaud 1992). In our studies the participation of I_f in the total inward current was deduced from: a) the presence of a low-threshold "hump" on the corresponding I/V-curve (between −80 and −45 mV); b) the ne-

gative shift of this curve at $V_h = -90$ mV as compared to the one obtained at $V_h = -50$ mV, both in Ba^{2+}- and Ca^{2+}- containing media (Figs. 2 and 3); c) the presence of a fast-inactivating I_{Ca} component, which was nifedipine-resistant and could be effectively blocked by Ni^{2+} from the outside (Fig. 3); d) it can be inferred from the data presented in Fig. 6 that the inactivation of I_f is potential, but not $Ca^{2+}{}_i$dependent, since its time constants of inactivation were almost identical both in Ca^{2+} and Ba^{2+} (Fig. 6*A*). It was also shown that I_f is not carried by Na^+ ions (see Fig. 4). According to Tsien's criteria (Tsien 1983), the above data suggests the coexistence of T- and L-types Ca^{2+}-channels in CC.

Steady-state inactivation of I_f and I_s. Since nifedipine did not affect the amplitde and inactivation kinetics of I_f, and at $V_h = -50$ mV I_s was totally blocked by nifedipine, the attempt to obtain h_∞-curve for I_f in the presence of this drug seemed reasonable. The resulting h_∞-curve for I_f seemed to reflect its real inactivation process, at least when compared to the data obtained in vascular muscle (Wang et al. 1989), gastric muscle (Walsh and Singer 1987), or urinary bladder (Isenberg and Klockner 1985).

Current through L-channels was found to inactivate more rapidly in Ca^{2+} than in Ba^{2+}, possibly because of the Ca^{2+}-dependent inactivation of L-channels which have been well described in many different cells (Isenberg and Klockner 1985; Amedee et al. 1987; Ganitkevich et al. 1991; Vogalis and Sanders 1991). However, our data also indicate a voltage dependent inactivation in these cells: a) there was a substantial amount of inactivation of I_s at potentials prior to activation of the L-current (Fig. 7); b) in Ca^{2+}-free solution, the outward current through Ca^{2+}-channels still inactivated; c) Ba^{2+} did not totally prevent I_s inactivation. In summary, these data suggest that the inactivation mechanism of the current through L-type Ca^{2+}-channels is both voltage- and Ca^{2+}-dependent.

Charge carrier. The absence of an inward current carried by Na^+ in CC is well documented in a nominally Ca^{2+}-free solution. The outward current observed in Ca^{2+}-free medium is most likely carried by Cs^+ from the pipette solution. Such a conclusion is consistent with the widespread opinion according to which monovalent cations are readily transported through Ca^{2+}-channels except when at least one channel binding site is occupied by Ca^{2+} (Hess and Tsien 1984, Bonev and Boev 1991).

Capacitance and current density The average cell capacitance reported here for CC is compatible with values measured in similar cell types (Yamamoto et al. 1989; Vogalis and Sanders 1991). The relatively high values of estimated current densities are consistent with measurements of Isenberg and Klockner (1985) and Yamamoto et al. (1989) in other smooth muscle cells, performed under very similar conditions (use of "KB" solution, 30–32 °C, slow "run-down" of the L-type Ca^{2+} channels).

Possible role of multiple types of Ca^{2+}-channels. The CC maintain more negative V_r than do cells from the ileal longitudinal layer, at least among the majority of animal species studied (Hara et al. 1986). Based on this it is assumed that the low-threshold Ca^{2+} channels may be responsible for the initial depolarization phase of the slow-wave type action potentials, conducting Ca^{2+} at membrane voltages close to the V_r of these cells.

Acknowledgements. We thank the Alexander von Humboldt Foundation for their gift of a TL-1 Labmaster interface and the pCLAMP software. This work has been supported by the Ministry of Science and Higher Education of Bulgaria, grant No B-11.

References

Amedee T., Mironneau C., Mironneau J. (1987): The calcium channel current of pregnant rat single myometrial cells in short-term primary culture. J. Physiol. (London) **392,** 253—272

Benham C. D., Hess P., Tsien R. W. (1987): Two types of calcium channels in single smooth muscle cells from rabbit ear artery studied with whole-cell and single-channel recordings. Circ. Res. **61,** Suppl. **1,** 10—16

Bolton T. B., Pacaud P. (1992): Voltage-dependent calcium channels in smooth muscle. Jpn. J. Pharmacol.**58,** Suppl. II, 251P—257P

Bonev A., Boev K. (1991): Two types of calcium channels in single smooth muscle cells from cat gastric antrum. Gen. Physiol. Biophys. **10,** 95—100

Droogmans G., Callewaert G. (1986): Ca^{2+}-channel current and its modification by the dihydropyridine agonist BAY K 8644 in isolated smooth muscle cells. Pflügers Arch. **406,** 259—265

Duridanova D., Gagov H., Boev K. (1992): Ionic currents in guinea-pig ileal smooth muscle - differences between single cells from longitudinal and circular layers. Comptes Rendus Acad. Bulg. Sci. **45,** No 12 (in press)

Ganitkevich V. Ya., Shuba M. F., Smirnov S. V. (1991): Inactivation of calcium channels in single vascular and visceral smooth muscle cells of the guinea-pig. Gen. Physiol. Biophys. **10,** 137—161

Hamill O. P., Marty A., Neher E., Sakmann B., Sigworth F. J. (1981): Improved patch-clamp techniques for high resolution current recording from cells and cell-free membrane patches. Pflügers Arch. **391,** 85—100

Hara Y., Kubota M., Szurszewski J. H. (1986): Electrophysiology of smooth muscle of the small intestine of some mammals. J. Physiol. (London) **372,** 501—520

Hess P., Tsien R. W. (1984): Mechanism of ion permeation through calcium channels. Nature **309,** 453—456

Isenberg G., Klockner U. (1982): Calcium tolerant ventricular myocytes prepared by preincubation in a "KB" medium. Pflügers Arch. **359,** 6—18

Isenberg G., Klockner U. (1985): Calcium currents of smooth muscle cells, isolated from the urinary bladder of the guinea-pig: inactivation, conductance and selectivity is controlled by micromolar amounts of $[Ca^{2+}]_o$. J. Physiol. (London) **358,** 60P

Isenberg G., Wendt-Gallitelli M. F., Ganitkevich V. (1992): Contribution of Ca^{2+}-induced Ca^{2+} release to depolarization-induced Ca^{2+} transients of myocytes from guinea-pig urinary bladder. Jpn. J. Pharmacol. **58,** Suppl. II, 81P—86P

Miyoshi H., Urabe T., Fujiwara A. (1991): Electrophysiological properties of membrane currents in single myometrial cells isolated from pregnant rats. Pflügers Arch. **419,** 386—393

Nakazawa K., Saito H., Matsuki N. (1988): Fast and slow inactivating components of Ca-channel current and their sensitivities to nicardipine in isolated smooth muscle cells from rat vas deferens. Pflügers Arch. **411,** 289—295

Nilius B., Hess P., Lansman J. B., Tsien R. W. (1985): A novel type of cardiac calcium channels in ventricular cells. Nature **334,** 443—446

Nowycky M. C., Fox A. P., Tsien R. W. (1984): Two components of calcium channel current in chick dorsal root ganglion cells. Biophys. J. **45,** 36a

Pelzer D., Pelzer S., McDonald T. F. (1990): Properties and regulation of calcium channels in muscle cells. Rev. Physiol. Biochem. Pharmacol. **114,** 108—207

Post J. M., Hume J. R. (1992): Ionic basis for spontaneous depolarizations in isolated smooth muscle cells of canine colon. Amer. J. Physiol. **263,** 3, part 1, C691—C699

Somlyo A. P., Somlyo A. V. (1992): Pharmacomechanical coupling: the role of G-proteins in Ca^{2+}-release and modulation of Ca^{2+}-sensitivity. Jpn. J. Pharmacol. **58,** (suppl. II), 54P—59P

Spedding M., Kenny B. (1992): Voltage-dependent calcium channels: structures and drug-binding sites. Biochem. Soc. Trans. **20,** 147—154

Suzuki M., Muraki K., Imaizumi Y., Watanabe M. (1992): Cyclopiazonic acid, an inhibitor of the sarcoplasmic reticulum Ca^{2+}-pump, reduces Ca^{2+}-dependent K^+ currents in guinea-pig smooth muscle cells. Brit. J. Pharmacol. **107,** 134—140

Tsien R. W. (1983): Calcium channels in excitable cell membranes. Annu. Rev. Physiol. **45,** 341—358

Vogalis F., Sanders K. M. (1991): Characterization of ionic currents of circular smooth muscle cells of the canine pyloric sphincter. J. Physiol. (London) **436,** 75—92

Walsh J. V., Singer J. J. (1987): Identification and characterization of major ionic currents in isolated smooth muscle cells using the voltage-clamp technique. Pflügers Arch. **408,** 83—97

Wang R., Karpinski E., Pang P. K. T. (1989): Two types of calcium channels in isolated smooth muscle cells from rat tail artery. Amer. J. Physiol. **256,** H1361—H1368

Ward S. M., Keller R. G., Sanders K. M. (1991): Structure and organization of electrical activity of canine distal colon. Amer. J. Physiol. **260,** G724—G735

Yamamoto Y., Hu S. L., Kao C. Y. (1988): Demonstration of multiple types of calcium channels in smooth muscle cells of the guinea-pig taenia coli. Biophys. J. **53,** 594a

Yamamoto Y., Hu S. L., Kao C. Y. (1989): Inward current in single smooth muscle cells of the guinea-pig taenia coli. J. Gen. Physiol. **93,** 521—550

Yoshino M., Yabu H. (1985): Single Ca channel currents in mammalian visceral smooth muscle cells. Pflügers Arch. **404,** 285—286

Yoshino M., Someya T., Nishino A., Yabu H. (1988): Whole-cell and unitary Ca channel currents in mammalian intestinal smooth muscle cells: evidence for the existence of two types of Ca channels. Pflügers Arch. **411,** 229—231

Zholos A. V., Baidan L. V., Shuba M. F. (1992): Some properties of Ca^{2+}-induced Ca^{2+} release mechanism in single visceral smooth muscle cells of the guinea-pig. J. Physiol. (London) **457,** 1—25

Final version accepted May 24, 1993